Thermal Infrared Remote Sensing for Urban Climate and Environmental Studies: An Application for the City of Bangkok, Thailand
การสำรวจระยะไกลด้วยข้อมูลอินฟราเรดความร้อนเพื่อการศึกษาภูมิอากาศและสิ่งแวดล้อมเมืองกับการประยุกต์ใช้ในพื้นที่กรุงเทพมหานคร

Manat Srivanit[1] and Kazunori Hokao[2]
มานัส ศรีวณิช[1] และ คาซูโนริ โฮเกา[2]

[1] Faculty of Architecture and Planning, Thammasat University, Pathumthani, 12121, Thailand
คณะสถาปัตยกรรมศาสตร์และการผังเมือง มหาวิทยาลัยธรรมศาสตร์ จังหวัดปทุมธานี 12121
E-mail: s.manat@gmail.com

[2] Department of Civil Engineering and Architecture, Graduate School of Science and Engineering, Saga University, 840-8502 Saga, Japan

Abstract

Thermal infrared remote sensing has been used over urban areas to assess urban heat islands (UHI), to perform land cover classifications and as input for models of urban surface atmosphere exchange. In this study, we review the use of thermal remote sensing in the study of urban climates, focusing primarily on the urban heat island effect and an integrated remote sensing-based approach to investigate the influences of urbanization on urban thermals and environment in Bangkok metropolitan area (BMA), Thailand. Three Landsat TM images, acquired in 1994, 2000 and 2009, were selected to retrieve the surface urban heat island (SUHI). Our analysis showed that higher temperatures in the SUHI were located with a scattered urban pattern, which was related to certain land-cover types. It was found that average surface temperature (Mean ± S.D.) in the BMA was about 26.01 ± 5.89°C degrees in 1994, but this difference jumped to 37.76 ± 2.84°C in 2000 and further to 39.79 ± 2.91°C in 2009, respectively. This could lead to an intensified urban heat island effect in the urban areas. The results of this study can provide methods and basic information for the reduction of urban temperature and the establishment of environmentally friendly urban planning. Overall, remote sensing technology was an effective approach for monitoring and analyzing urban growth patterns and evaluating their impacts on urban climates.

บทคัดย่อ

การสำรวจระยะไกลด้วยข้อมูลอินฟราเรดความร้อนถูกนำไปใช้กับพื้นที่เมืองในการประเมินปรากฏการณ์ เกาะความร้อนเมือง ยังถูกนำไปประกอบในกระบวนการจำแนกสิ่งปกคลุมดินและเป็นปัจจัยในการนำเข้าแบบจำลองการแลกเปลี่ยนบรรยากาศพื้นผิวในพื้นที่เมือง ในการศึกษานี้ ได้พิจารณาใช้ค่าความร้อนจากการสำรวจระยะไกลในการศึกษาสภาพภูมิอากาศในเขตเมือง โดยมุ่งศึกษาถึงผลกระทบของปรากฏการณ์เกาะความร้อนเมืองและบูรณาการตามวิธีการสำรวจระยะไกลเพื่อศึกษาอิทธิพลของกระบวนการกลายเป็นเมืองที่มีต่ออุณหภูมิและสิ่งแวดล้อมเมือง ในเขตพื้นที่กรุงเทพมหานคร ด้วยการเลือกใช้ประโยชน์จากข้อมูลภาพถ่ายดาวเทียมแลนด์แซท ทีเอ็ม สามช่วงเวลาในปี 1994, 2000

และ 2009 เพื่อประเมินปรากฏการณ์เกาะความร้อนพื้นผิวเมือง จากการวิเคราะห์ พบว่า อุณหภูมิที่สูงของความร้อนพื้นผิวเมืองมีรูปแบบกระจัดกระจายไปตามพื้นที่ต่าง ๆ โดยมีความสัมพันธ์มากกับประเภทของสิ่งปกคลุมดิน พบว่า อุณหภูมิพื้นผิวเฉลี่ย (ค่าเฉลี่ย ± ค่าส่วนเบี่ยงเบนมาตรฐาน) ในกรุงเทพมหานครมีค่าประมาณ 26.01 ± 5.89 องศาเซลเซียส ในปี 1994 ความแตกต่างนี้ได้เพิ่มขึ้นไปเป็น 37.76 ± 2.84 องศาเซลเซียส ในปี 2000 เพิ่มขึ้นอย่างต่อเนื่องเป็น 39.79 ± 2.91 องศาเซลเซียส ในปี 2009 ตามลำดับ โดยจะทวีความรุนแรงของผลกระทบจากปรากฏการณ์เกาะความร้อนเมืองมากขึ้นในเขตพื้นที่เมือง ผลการศึกษาครั้งนี้สามารถนำไปเป็นข้อมูลพื้นฐานเพื่อนำมาสู่การกำหนดมาตรการลดอุณหภูมิเมืองและการวางผังเมืองที่เป็นมิตรกับสิ่งแวดล้อมต่อไป ทั้งนี้ เทคโนโลยีการสำรวจระยะไกล หรือรีโมตเซนซิง เป็นวิธีการที่มีประสิทธิภาพสำหรับการตรวจสอบและวิเคราะห์รูปแบบการเติบโตของเมืองและการประเมินผลกระทบที่มีต่อสภาพภูมิอากาศในเขตพื้นที่เมือง

Keywords

Remote Sensing (การสำรวจระยะไกล)
Urban Heat Island: UHI (เกาะความร้อนเมือง)
Surface Urban Heat Island: SUHI (เกาะความร้อนพื้นผิวเมือง)
Land Surface Temperature: LST (อุณหภูมิพื้นผิว)
LANDSAT TM (ดาวเทียมแลนด์แซท ทีเอ็ม)

1. Introduction

Surface temperature is of prime importance to the study of urban climatology. It modulates the air temperature of the lowest layers of the urban atmosphere, is central to the energy balance of the surface, helps to determine the internal climates of buildings and affects the energy exchanges that impact on the comfort of city dwellers. Surface and atmospheric modifications due to urbanization generally lead to a modified thermal climate that is warmer than the surrounding non-urbanized areas, particularly at night. This phenomenon is the urban heat island (UHI) (Voogt & Oke, 2003, pp. 370-384). Heat islands can be characterized according to different layers of the urban atmosphere and for various surfaces and divided into three categories (Figure 1): canopy layer heat island (CLHI), boundary layer heat island (BLHI), and surface urban heat island (SUHI). The urban canopy layer extends upwards from the surface to approximately mean building height, whereas the urban boundary layer is located above the canopy layer (Voogt & Oke, 2003, pp. 370-384). The CLHI and the BLHI are atmospheric heat islands since they denote a warming of the urban atmosphere, whereas the SUHI refers to the relative warmth of urban surfaces compared to surrounding rural areas.

It is known that atmospheric UHIs are larger at night while surface UHIs are larger during the day (Roth, Oke & Emery, 1989, pp. 1699-1720). While

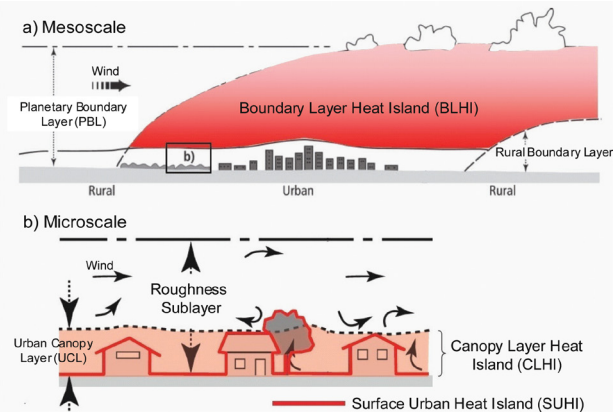

Figure 1. Schematic depiction of the main components of the urban atmosphere (Modified after Voogt, 2004).

atmospheric heat islands are normally measured by in situ sensors of air temperature via weather station networks, the SUHI is typically characterized as land surface temperature (LST) through the use of airborne or satellite thermal infrared remote sensing, which provides a synoptic and uniform means of studying SUHI effects at regional scales. Satellite-measured LST is a key parameter in SUHI processes, not only acting as a indicator of climate change, but also due to its control of the upward terrestrial radiation, and consequently, the control of the surface sensible and latent heat flux exchange with the atmosphere (Aires, Prigent, Rossow & Rothstein, 2001, pp. 14887-14907; Sun & Pinker, 2003, pp. 4326-4241). Thus, the surface temperatures have an indirect but significant influence on air temperatures. For example, parks and vegetated areas, which typically have cooler surface temperatures, contribute to lower air temperatures. Dense built-up areas, on the other hand, typically lead to warmer air temperatures. Bangkok, like other Asian cities, continues to rapidly grow in both its population and physical size. Consequently, the study of surface urban heat island will become progressively more important for researchers and decision makers to understand the climate effects of urbanization in order to contribute to sustainable urban development in the region.

The definition of remotely sensed variables is important in order to understand precisely the information content of remotely sensed quantities and how they relate to actual surface properties. Thermal remote sensing of urban surface temperatures is a special case of observing land surface temperature which varies in response to the surface energy balance. The resultant surface temperature incorporates the effects of surface radiative and thermodynamic properties including; surface moisture, thermal admittance and surface emissivity –the radiative input at the surface from the sun and atmosphere, and the effects of the near-surface atmosphere and its relation to turbulent transfer from the surface (Figures 2).

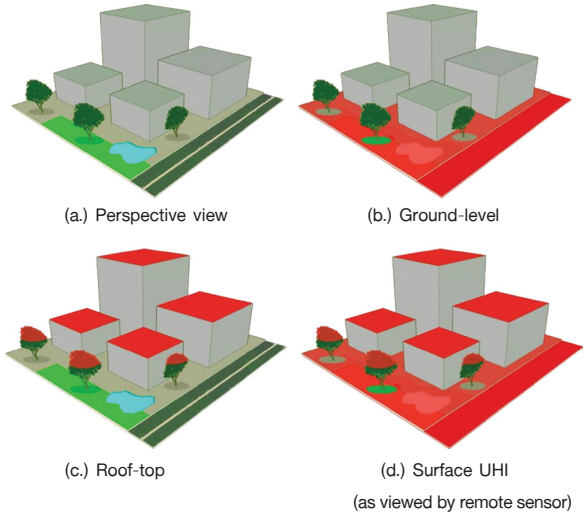

Figures 2. Schematic illustration of definitions of the Surface Urban Heat Island (SUHI) as observed by a remote sensor (Modified after Voogt & Oke, 2003).

Remotely sensed thermal infrared (TIR) data have been widely used to retrieve land surface temperature (LST) (Quattrochi & Luvall, 1999, pp. 577-598; Weng & Schubring, 2004, pp. 16-26). A series of satellite and airborne sensors have been developed to collect TIR data from the earth surface, such as HCMM, Landsat TM/ETM+, AVHRR, MODIS, ASTER, and TIMS. In addition to LST measurements, these TIR sensors may also be utilized to obtain emissivity data of different surfaces with varied resolutions and accuracies. LST and emissivity data are used in urban climate and environmental studies, mainly for analyzing LST patterns and its relationship with surface characteristics, for assessing surface urban heat island (SUHI), and for relating LSTs with surface energy fluxes in order to characterize landscape properties, patterns, and processes (Quattrochi & Luvall, 1999, pp. 577-598). Remotely sensed TIR data are a unique source of information to define surface heat islands, which are related to canopy layer heat islands. In situ data (in particular, permanent meteorological station data) offer high temporal resolution and long-term coverage but lack spatial details. Moving observations overcome this limitation to some extent, but do not provide a synchronized view over a city. Only remotely sensed TIR data provide a continuous and simultaneous view of the whole city, which is of prime importance for a detailed investigation of urban surface climate.

The first SUHI observations (from satellite-based sensors) were reported by Rao (1972), demonstrating that urban areas could be identified from the analyses of thermal infrared data acquired by a satellite. Gallo et al. (1995) reviewed and represented a satellite perspective on the assessment of SUHI. Studies on the SUHI phenomenon using satellite derived land surface temperature (LST) measurements have been conducted primarily using NOAA AVHRR data (Gallo & Owen, 1998a, pp. 35-41, 1998b, pp. 806-813; Streutker, 2002, pp. 2595-2608) for regional-scale urban temperature mapping. Recently, Landsat Thermatic Mapper (TM) and Enhanced Thermatic Mapper Plus (ETM+) thermal infrared (TIR) data with 120 m and 60 m spatial resolutions, respectively, have also been utilized for local-scale studies of UHI (Chen, Wang & Li, 2002; Weng, 2001, pp. 1999-2014).

Remotely sensed LST records the radiative energy emitted from the ground surface, including building roofs, paved surfaces, vegetation, bare ground, and water (Arnfield, 2003, pp. 1-26; Voogt & Oke, 2003, pp. 370-384). Therefore, the pattern of land cover in urban landscapes may potentially influence LST (Arnfield, 2003, pp. 1-26; Forman, 1995). The two fundamental aspects of land cover pattern are composition and configuration (Gustafson, 1998, pp.143-156; Turner, 2005, pp. 319-344). Composition refers to the abundance and variety of land cover features without considering their spatial character or arrangement (Gustafson, 1998, pp. 143-156; Leitao, Miller, Ahern & McGarigal, 2006). Configuration, in contrast, refers to the spatial arrangement or distribution of land cover features. In addition to influencing LST through direct modification of surface characteristics, land cover pattern may also influence LST through its affects on the movements and flows of organisms, material, and energy in a landscape (Forman, 1995; Turner, 2005).

Previous SUHI research has primarily focused on the effects of land cover composition, especially vegetation abundance, on LST (e.g. Buyantuyev & Wu, 2010; Frey, Rigo & Parlow, 2007; Weng, Lu & Schubring, 2004; Weng, 2009). Remotely sensed data has typically been used to evaluate LST patterns and assess the UHI, especially at vast geographic scales. Using a variety of image data, including NOAA AVHRR (Balling & Brazell, 1988, pp. 1289-1293), MODIS (Pu, Gong, Michishita & Sasagawa, 2006, pp. 211-225), Landsat TM/ETM+ (Weng et al., 2004), ASTER (Lu & Weng, 2006; Pu et al., 2006) and airborne ATLAS (Lo, Quattrochi & Luvall, 1997, pp. 287-304), these studies show that surface cover characteristics, such as vegetation abundance measured by NDVI (Normal Difference Vegetation Index), and the relative amounts of types of land use/land cover, significantly affect LST in urban areas (e.g. Buyantuyev & Wu, 2010; Liang & Weng, 2008; Weng, 2003; Weng et al., 2004; Xiao et al., 2008).

The purpose of this study is to understand impacts of urbanization on local climate and assess the diurnal and seasonal variation of the surface urban heat island intensity (SUHI), measured from the thermal infrared of Landsat TM satellite images in BMA, using remote sensing images of different time periods and then analyzing the surface temperature retrieved from the thermal infrared band. In this paper, multi-temporal Landsat TM imagery of 1994, 2000, and 2009 were used to investigate the impact of such changes on the intensity and spatial pattern of the SUHI effect in BMA. In the last part of the paper, the authors share their viewpoint on research trends in thermal remote sensing of urban areas, and provide updates on current and future TIR remote sensors.

2. The Study Area

Bangkok (center latitude: 13° 33' 44.37"N, center longitude: 100° 38' 47.76"E) has been the capital city of Thailand for more than 200 years, situated on flat low land in the southern part of the Lower Central Plain of the country. The Chao Phraya River flows through the city from the northern highland and discharges into the Gulf of Thailand, 25 km south of the city. The metropolis of Bangkok has gradually grown up into one of the world's populated cities with a registered population of over 5.5 million and estimated actual population of up to 10 million on the 1,576 sq.km area (the Bureau of Registration Department, 2004). Bangkok Metropolitan Administration has divided the city into three zones (inner, middle, and outer) in accordance with the population density. Bangkok is subdivided into 50 districts, with 21 (207 sq.km. area), 18 (485 sq.km area) and 11 (884 sq.km. area) in the inner, middle and outer zones respectively.

As an economic magnet, Bangkok's population is continually increasing through in-migration from the Thai countryside. This rapid rise in population, capital investment, factories and employees in Bangkok has accelerated the development of road networks, real estate developments, land value and advanced technologies, resulting in expansion of the city to the surrounding areas. Besides a number of other environmental problems, such as air pollution, water pollution, and land subsidence, this rapid urbanization has also led to urban heat island effects. Furthermore, as the city has continued to grow in both population and physical size, these urban–rural differences in temperature have also increased, as reported by long-term temperature records. Boonjawat et al. (2000) found an increase of 1.23°C in lowest air temperature in the UHI of Bangkok over the last 50 years. The peak temperature of metropolitan areas such as Bangkok can be higher than the surroundings by 3.5 °C, as detected during clear and calm nights in the dry season. Increased temperatures due to the UHI effect may increase water consumption and energy use in urban areas and lead to alterations to biotic communities (White, Nemani, Thornton & Running, 2002, pp. 260-277). Kiattiporn et al. (2008) found that a temperature

increase of 1°C will result in a 6.79% increase in electricity consumption in the BMA. Excess heat may also affect the comfort of urban dwellers and lead to greater health risks (Poumadere, Mays, LeMer & Blong, 2005, pp. 1483-1494). In addition, higher temperatures in urban areas increase the production of ground level ozone which has direct consequences for human health (Akbari, Rosenfeld, Taha & Gartland, 1996; Akbarietal, 2001). It is, therefore, important to analyze the impacts of urbanization on SUHI in BMA and its relationship with urban surface temperature in order to lessen the ever worsening urban climate problem in the region.

A total of 14 weather stations were used to acquire air temperatures (Figure 3 and Table 3) and a variety of sources can be used to take these measurements, including stations operated by the Thai Meteorological Department (TMD), the Pollution Control Department (PCD), the Thai Red Cross Society (TRC) and the Nakhonthai Automatic Weather Station Network (NTN). These stations were equipped with a temperature sensor and were mounted at a 1.5-2.0 m height in a ventilated shelter protected against solar radiation and precipitation. For investigating the temporal characteristics of the urban heat island intensity (UHII) in the BMA, two meteorological stations were selected: (1) Ploenchit Station (TRC1), a fixed station near the urban core, to represent urban conditions; and (2) Phasi Charoen station (NTN2), located in the western part of the BMA, to represent suburban or rural conditions in Bangkok. It was envisaged that comparisons of the readings of these stations during a period of 1 year (January to December, 2009) could yield reliable indicators of the daily development of thermal differences between rural and urban areas.

The summer period, or hot and humid season, is from March to June. At this time, temperatures in BMA average around 39 °C, but April has the highest solar intensity and longest days. During this season it can therefore become quite hot (Figure 4a), thus affecting the community environment and quality of life. The monthly average heat island intensities are illustrated in Figure 4b; the average maximum UHII over the 1-year period is 4.3°C. However, evaluation of readings of UHII discloses clear cycles. Diurnally, it is stronger during nighttime (18:00-07:00 hours) than during daytime (07:00-18:00 hours). Seasonally, the analysis indicates that urban heat intensity tends to be strong in winter (from November to February); the strongest can be found at nighttime in January and the weakest in the summer. Figure 5a and Figure 5b show the typical temporal variations of urban and rural air temperature under clear skies and weak airflow on 4^{th}-5^{th} January, 2009. The strength of the UHII is referred to by the maximum difference recorded. The magnitude of $\Delta T_{u\text{-}r}$ is greatest at night, under clear skies and with little wind. Under such conditions, surface cooling is associated with radiation exchange. While exposed rural sites cool rapidly after sunset, urban sites cool more slowly. The difference between urban and rural sites grows with time after sunset and reaches a maximum difference after about 4-5 hours.

During the winter season, the UHII can reach a maximum of 7.0°C during nighttime in January and a minimum of 2.2°C during the afternoon in February (12:00-18:00 hours). Except in August, the nocturnal range of the UHII seems to be about the same as in the afternoon. During the wet months between July and October, the nocturnal range and day heat island intensity is less pronounced, especially in August, reaching a minimum of around 4.4°C. The diurnal range of seasonal variation of the urban heat island seems to be related to the seasonal variations in the incoming solar radiation. The monthly mean of the solar radiation in Bangkok exceeded 144 W/m^2 in April. These large values of average solar radiation and the seasonal variations directly affect the amount and seasonal variations of the heat trapped by urban surfaces. As a result of such variation, the SUHI are typically largest in the summer.

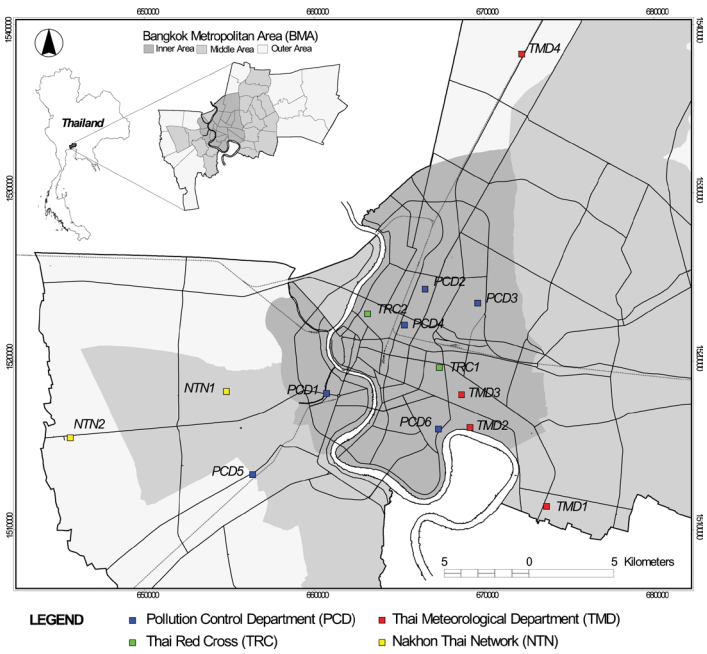

Figure 3. Location of the Bangkok Metropolitan Area (BMA) and location of the reference weather stations used in the analysis.

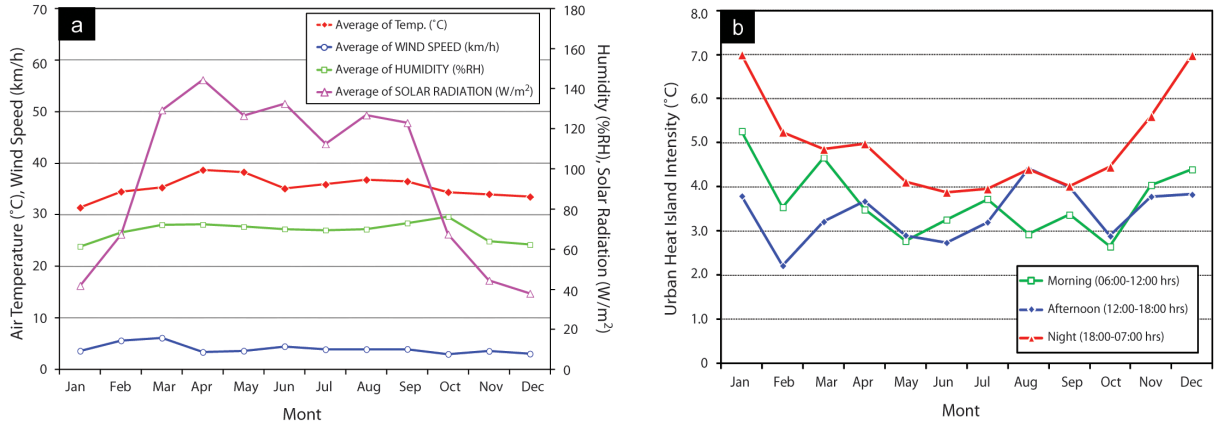

Figures 4. (a.) Urban climatic characteristics in 2009 of Bangkok (the reference station at Ploenchit Station (TRC1)), and (b.) Seasonal variation of monthly average the urban heat island intensity between urban (TRC1) and rural (NTN2) stations for three periods in 2009.

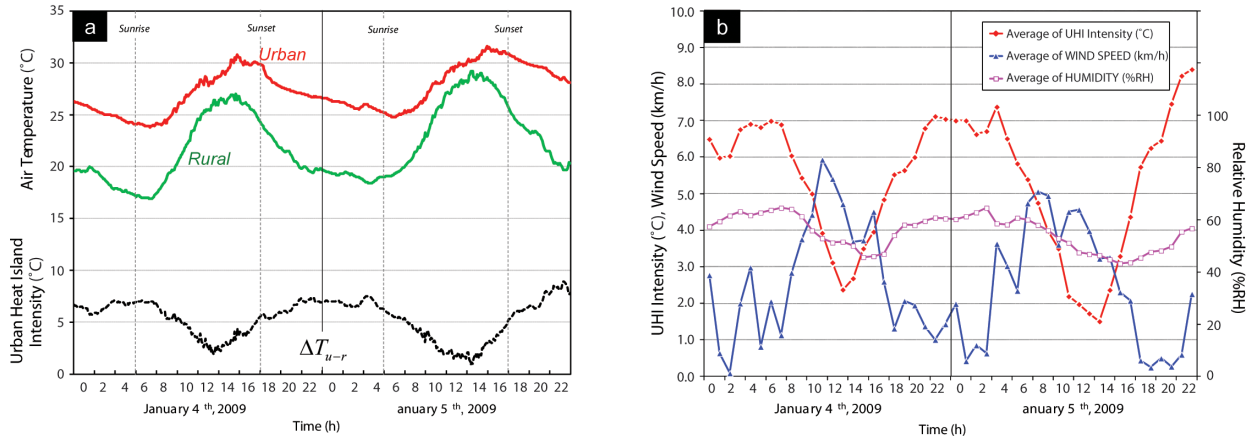

Figures 5. (a.) Typical temporal variation of urban (TRC1) and rural (NTN2) air temperature under clear skies and weak airflow and (b.) The urban heat island intensity, wind velocity and relative humidity on 4th-5th January, 2009.

3. Methods

3.1 Image Pre-processing

Landsat data from three different years were obtained. Landsat thematic mapper (TM) images acquired on March 5th, 1994 (the early summer), February 18th, 2000 (the late winter) and April 25th, 2009 (the summer) were geo-referenced to a common UTM coordinate system based on the rectified high resolution QuickBird image, aerial photograph and the 1:50,000 scale topographic maps. Using the radiometric correction method of Schroeder et al. (2006), the original digital numbers of bands 1–5 and 7 images were converted to at-satellite radiance, at-satellite reflectance, and then to surface reflectance. While bands 1 through 5 and band 7 are at a spatial resolution of 30 m., the thermal infrared band (band 6) comes at an original spatial resolution of 120 m. for Landsat 5 TM images.

3.2 Derivation of LST from Landsat TM Imageries

LST is the radiative skin temperature of the land surface, which plays an important role in the physics of the land surface through the process of energy and water exchanges with the atmosphere. The derivation of LST from satellite thermal data requires several procedures: sensor radiometric calibrations, atmospheric and surface emissivity corrections, characterization of spatial variability in land-cover, etc. As the near-surface atmospheric water vapour content varies over time due to seasonality and inter-annual variability of the atmospheric conditions, it is inappropriate to directly compare temperature values represented by the LST between multiple periods. Therefore the focus here is on the surface urban heat island intensity (SUHII) and its spatial patterns across the study region. SUHII is estimated as the difference between the peak surface temperatures of the urban area and the background non-urban temperatures (Chen, Zhao, Li & Yin, 2006). This SUHI effect can be determined for the individual thermal images and then compared between two or more periods. However, before we compute the SUHI effect, we must first derive the LST based on methods for ETM+ images.

As described above, the Landsat TM thermal infrared band (10.4–12.5 μm) data were used to derive the LST. Yuan, Sawaya, Loeffelholz & Bauer (2005) proposed a method of deriving LST in three steps. Firstly, the digital numbers (DNs) of band 6 are converted to radiation luminance or top-of-atmospheric (TOA) radiance (L_λ, mW/(cm^2 sr·μm) using (Eq. [1]) (Chander & Markham, 2003, pp. 2674-2677):

$$L_\lambda = \frac{(L_{max} - L_{\min})}{QCAL_{max} - QCAL_{\min}} \times (DN - QCAL_{\min}) + L_{\min} \quad [1]$$

Where *DN* is the pixel digital number for band 6, $QCAL_{\max}$ = 255 is the maximum quantized calibrated pixel value corresponding to $L_{\max}$, $QCAL_{\min}$ = 0 is the minimum quantized calibrated pixel value corresponding to $L_{\min}$, $L_{\max}$ = 17.04 (mW/cm^2 sr·μm) is spectral at-sensor radiance that is scaled to $QCAL_{\max}$ and $L_{\min}$ = 0 (mW/cm^2 sr·μm) is spectral at-sensor radiance that is scaled to $QCAL_{\min}$.

Secondly, the radiance was converted to surface temperature using the Landsat specific estimate of the Planck curve (Eq. [2]) (Chander & Markham, 2003, pp. 2674-2677):

$$T_k = \frac{K2}{In\left(\frac{K1}{L_\lambda} + 1\right)} \quad [2]$$

Where T_k is the temperature in Kelvin (K), $K1$ is the prelaunch calibration of constant 1 in unit of W/(m^2 sr·μm) and $K2$ is the prelaunch calibration constant 2 in Kelvin. For Landsat TM, $K1$ is about 607.76 W/(m^2 sr·μm) and is about 1260.56 W/(m^2 sr·μm) with atmospheric correction (Barsi et al., 2003). The final apparent surface temperature in Celsius (°C) can be calculated using the following equation:

$$T_c = T_k - 273.15 \quad [3]$$

Where T_c is the temperature in Celsius (°C), T_k is the temperature in Kelvin (K).

4. Results and Disscussions

4.1 Spatial and Temporal Distribution Pattern of SUHI

The digital remote sensing method provides not only a measure of the magnitude of surface temperatures of the entire metropolitan area, but also the spatial extent of the surface heat island effects. In this study, we selected three Landsat images, i.e., the Landsat 5 TM images on March 5th, 1994, February 18th, 2000 and April 25th, 2009, respectively. It was found that average surface temperature (Mean ± S.D.) in the BMA was about 26.01 ± 5.89°C degree in 1994, but this difference jumped to 37.76 ± 2.84°C in 2000 and further to 39.79 ± 2.91°C in 2009, respectively. Figures 6 shows the increasing extent of SUHI over the study period. In 1994, the areas with higher surface radiant temperature were mainly located in the central urban areas and major districts, such as Don Mueang airport district and Khlong Toei port district, also known as Bangkok Port, Thailand's major hub for sea transportation of cargo–both areas with the typical strip shape associated with traffic road systems. Within the central urban area, numerous sub-centers of SUHI with higher surface radiant temperature were mainly located in the old and recently developed downtowns at the middle section of the Chao Phraya River (Figures 8).

The surface urban heat island intensity (SUHII) was defined as the maximum surface temperature difference between urban and suburban areas, measured from the Landsat images. The SUHII for three dates were listed in Table 1. From a maximum SUHII difference of 8.16°C between urban and rural areas in 1994, the difference jumped to 10.89°C in 2000 and rose further to 11.50°C in 2009, changes of 2.76°C and 0.61°C for the 1994–2000 and 2000–2009 periods, respectively.

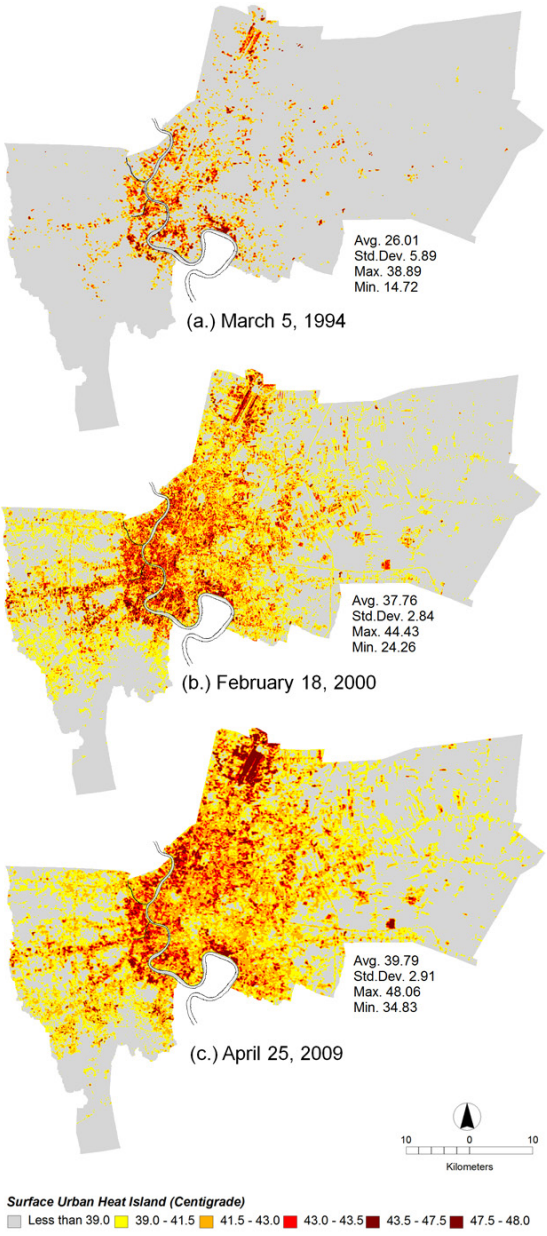

Figures 6. SUHI derived from Landsat TM (a, b, c) imagery for three different dates.

The results in Figures 8 and Figures 9 suggest that the spatial pattern of the SUHI (areas with relatively high temperatures) has changed from a scattered pattern (bare land, semi-bare land and urban area were warmer than other areas) in 1994 to a more contiguous pattern of urban heat islands in 2009, along with the expansion of the regional urban system. The centers of high temperature were consistent with built-up areas, which can be seen by comparing land use/cover with temperature maps: for example, in Figures 7a and 7b, which represent

the spatial distribution patterns of the SUHI in Bang Rak District on April 25th, 2009. On the right-hand side of both images is Lumphini Park; this park offers rare open public space, trees and playgrounds in the Thai capital and contains an artificial lake where visitors can rent a variety of boats. The park is noticeably cooler and demonstrates the impact that vegetated areas such as city parks can have on reducing diurnally thermal radiation, which contribute to cooler air temperatures. On the other hand, some hot spots, or SUHI, can be easily identified. The most extensive SUHI was distributed in the dense built-up areas, typically leading to warmer air temperatures.

The spatial distribution of SUHI was, to a large extent, in line with the pattern of impervious area. However, the distribution of SUHI in the urban core of 2009 was not as compact as that of 1994 due to the city's greening efforts and the decrease of heavy industries in this part of the city. SUHI area was mostly located at the places dominated by high-rise and low-rise residential buildings, commercial areas, industrial areas and bare soils, while the non-SUHI area mainly occurred around bodies of water and areas with moderate-to-high vegetation abundance, such as forests, crops or parks.

Table 2 shows the average SUHI for three dates by zone area of BMA. Overall, for the zone extent of average surface temperature from 1994 to 2009, the inner zone area (21 districts, 13.14% area of BMA) has the highest mean SUHI for 1994 and 2000, respectively, but in 2009 the mean SUHI is nearly the same as that of the middle and outer zone areas, with the value slightly over 39°C. This means that there is some homogenization and expansion of urban development over the study area in 2009, compared to 1994.

The standard deviation (S.D.) of SUHI is much larger in 1994 compared to 2009, although this difference in S.D. of SUHI could also be attributed to seasonal fluctuations of SUHI, as the mean SUHI and its S.D. in late winter (March 1994) would be expected to be less than the mean SUHI in summer

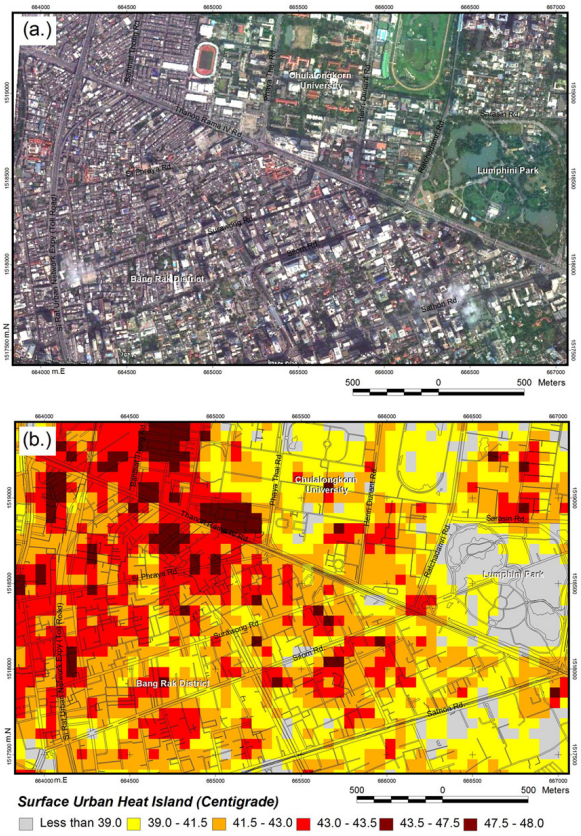

Figures 7. Spatial distribution patterns of the SUHI in the Bang Rak district (a.) Google map, and (b.) Surface temperature from the Landsat TM images acquired on April 25th, 2009 (the summer season).

Table 1. Descriptive statistics and the surface urban heat island intensity (SUHII) of study area for observed years

Statistics	SUHII 1994	SUHII 2000	SUHII 2009
Intensity of SUHI (°C)	8.16	10.89	11.50
Mean (°C)	26.01	37.76	39.79
Standard deviation (S.D.)	5.89	2.84	2.91

(April 2009). Explained in a different context, the S.D.s of SUHI are generally larger for the outer zone area than the inner zone area, indicating that the outer zone landscapes would have experienced wider variation in SUHI than the natural vegetation because of the mix of land use/land cover (LULC) types and different building structures and construction materials. This explains the thermal

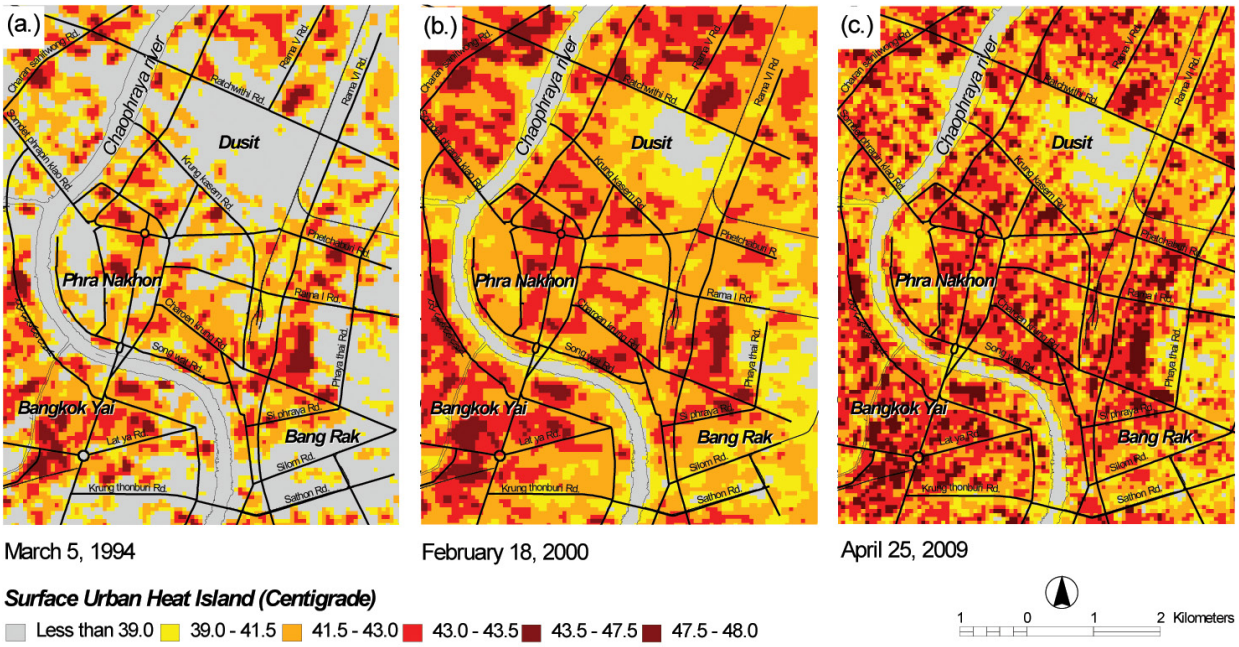

Figures 8. Spatial distribution patterns of the SUHI in the Rattanakosin Island (Phra Nakhon, Dusit, Bang Rak, Bangkok Yai District) from the Landst TM images acquired on (a.) 1994, (b.) 2000, and (c.) 2009.

heterogeneity that characterizes these areas. The S.D.s of SUHI are relatively small for the inner zone areas because of the homogeneity of construction types contributing to low SUHI variation in these areas.

In addition to urban expansion, there have been significant changes to the old parts of the cities. A great amount of land in those parts has been re-developed by the government or private companies for the construction of new residential, shopping, and industrial facilities. As a result, traditional wooden houses, rice straw roofs, and tile roofs were razed and replaced by skyscrapers and high buildings, which were constructed with non-evaporating, non-transpiring steel frames and concrete. The conversion of forest and agricultural land into urban/built-up land has also contributed to increased SUHI. The government has relocated many factories to industrial zones in the outskirts of the cities in order to make them more competitive. The new factories, along with supporting infrastructures, were frequently located in high-quality agricultural land or forestland, while old factories were abandoned and the land remained unused afterwards. This relocation has reduced agricultural areas and increased SUHI. In the past, agricultural or forest areas could provide a buffer zone between the urban and rural areas to absorb excess heat generated by automobiles and factories.

Table 2. Average SUHI (Mean ± S.D.) associated with zone of BMA.

Zone	SUHI 1994	SUHI 2000	SUHI 2009
Inner zone	36.81± 4.99°C	40.82±1.48°C	42.26±1.19°C
Middle zone	30.54±5.64°C	39.19±1.68°C	41.24±1.43°C
Outer zone	25.63±4.87°C	37.81±1.59°C	39.68±1.63°C

4.2 Relationships between the SUHI and Air Temperature

On a sunny summer day, the main cause of the urban climate is modification of the land surface by urban development which uses materials which effectively retain heat. Thus, surface temperature is an important condition for studies of the urban

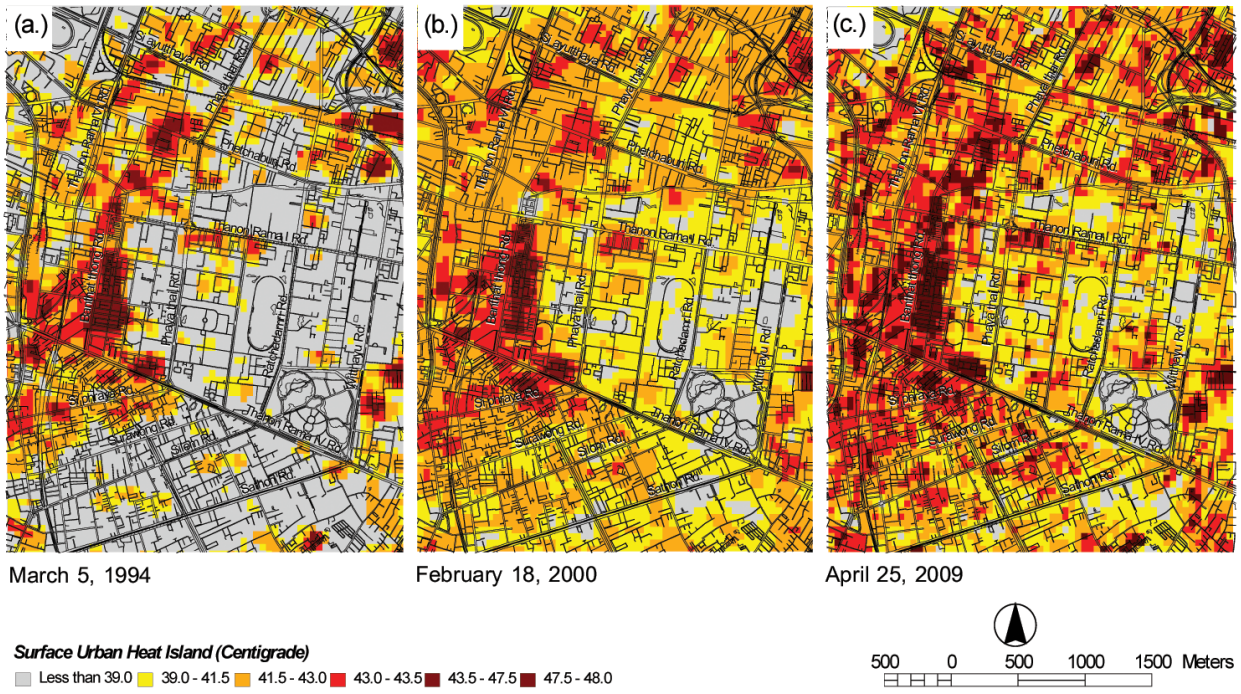

Figures 9. Spatial distribution patterns of the SUHI in the central business district area (Pathumwan, Bang Rak district) from the Landsat TM images acquired on (a.) 1994, (b.) 2000, and (c.) 2009

climatology. For this study, surface temperatures at the fourteen reference weather stations were extracted from surface temperature data. Figure 10b shows the relation between the air temperature obtained from weather stations and the surface temperature derived from the Landsat TM thermal image summer (April 25th, 2009; acquisition time 15:24:56-15:25:21 hours) at the weather stations. The simple linear regression lines were calculated to represent the relation between the air temperature and the surface temperature. It was found that the climate behaviors based on surface temperatures during the day are quite similar to those observed with the fixed weather stations' air temperature. Approximately 63.1% of the variation in the average air temperature closest to the acquisition time of satellite data was explained by the average surface temperature of the summer diurnal range within the *'Source area of temperature'* (also known as *the circle of influence*). An effective radiometric source area for a remote thermal measurement is the instantaneous field of view (IFOV) of the sensor projected onto the surface. For this study, all weather stations are defined by a circle of influence whose radius extends 300 meters, as recommended by Oke (2004) in the Initial Guidance to Obtain Representative Meteorological Observations at Urban Sites by World Meteorological Organization (Table 4). These results could be related to the findings of some studies (e.g. Ben-Dor & Saaroni, 1997; Nichol, 1994; Nichol, Fung, Lam & Wong, 2009), there is more consistent relationship between these two.

Among the different stations, it was found that the highest average surface temperature (Mean ± S.D.) in the Thonburi Power Substation (PCD1) station was about 43.41±0.82°C, followed by the Don Muang Airport (TMD4) and the Huaykwang National Housing Authority (PCD3) station at 42.90±0.92°C and 42.78 ± 0.40°C, respectively. These standard deviations (S.D.s) of surface temperature are relatively small, thus indicating that the homogeneity of construction types contributes to low surface temperature variation in these areas. The lowest average surface temperature site, at 40.49±1.16°C, was located at Nong Khaem

station (NTN1) station in the outskirts of the BMA and the S.D. of the surface temperature is much larger. Thus, it indicates that the landscapes would have experienced wider variation in surface temperature than the natural vegetation because of the mix of land use/land cover types and different building structures and construction materials. The average air temperatures in this area are also the lowest, indicating the contribution that vegetated areas make in reducing surface temperature.

After investigating the relation between air temperature and surface temperature, it became clear that the observed variation in air temperature could be explained by the surface temperature. A simple linear regression model [Eq.4] was developed using T_s as the independent variable and T_a as the dependent variable for all data points on April 25th, 2009:

$$T_a = 1.0332T_s - 12.775 \ (r^2 = 0.631, n=14) \qquad [4]$$

Where T_a is air temperature, T_s is average surface temperature derived from the Landsat TM thermal infrared image acquired on April 25th, 2009, n is the number of data points or the reference weather stations, and r^2 is the strength of the regression model. In this model, r^2 is 0.631, which means that 63.1 percent of the variation of the reference weather stations temperature can be explained by the SUHI data.

Table 3. Fourteen weather stations and derived parameters on April 25th, 2009

Station ID	Station Name	Location		Air Temp. (°C)	Surface Temperature (°C)*		
		Latitude	Longitude		Avg.±SD	Max.	Min.
TMD1	Bang Na	13°39'58.263"N	100°36'21.202"E	29.7	41.78±0.61	42.71	40.46
TMD2	Bangkok Port (Klong Toei)	13°42'31.541"N	100°33'52.301"E	31.8	42.73±1.54	44.67	38.44
TMD3	Sirikit Center	13°43'34.808"N	100°33'35.744"E	30.7	41.68±1.24	43.45	38.44
TMD4	Don Muang Airport	13°54'32.483"N	100°35'37.981"E	31.5	42.9±0.92	44.67	40.71
PCD1	Thonburi Power Substation	13°43'39.336"N	100°29'11.610"E	32.3	43.41±0.82	44.92	41.21
PCD2	Dindaeng National Housing Authority	13°46'59.348"N	100°32'25.750"E	30.2	41.83±0.91	42.71	39.2
PCD3	Huaykwang National Housing Authority	13°46'31.978"N	100°34'8.979"E	32	42.78±0.40	43.45	41.46
PCD4	Ministry of Science and Technology	13°45'50.161"N	100°31'44.681"E	30.2	42.44±0.65	43.45	40.71
PCD5	Singharaj Pittayakom School	13°41'3.153"N	100°26'45.554"E	30.8	42.25±0.51	43.2	41.21
PCD6	Nonsi Withaya School	13°42'28.905"N	100°32'50.376"E	31.6	42.7±0.36	43.94	41.96
TRC1	Ploenchit	13°44'27.601"N	100°32'52.786"E	31.2	41.64±1.20	42.71	37.93
TRC2	Suankularb Palace	13°46'12.341"N	100°30'33.112"E	29.5	42.16±0.64	43.2	40.71
NTN1	Nong Khaem	13°43'43.850"N	100°25'55.107"E	28.8	40.49±1.16	43.45	38.44
NTN2	Phasi Charoen	13°42'16.245"N	100°20'48.384"E	32.16	40.92±1.15	42.71	38.95

Note: *defined by a circle of influence whose radius extends 300 meters around the reference weather stations.

Table 4. Relationships between the average air temperature and the average surface temperature on April 25th, 2009 obtained by simple linear regression mode.

Variable Entered	*R*	R^2	$Adj.R^2$	*Std. Error of the Estimate*	*F*	*P-value*
The average surface temperature (T_s)	0.794	0.631	0.600	0.656	20.486	<0.001

Note: dependent indicator is the average air temperature (T_a)

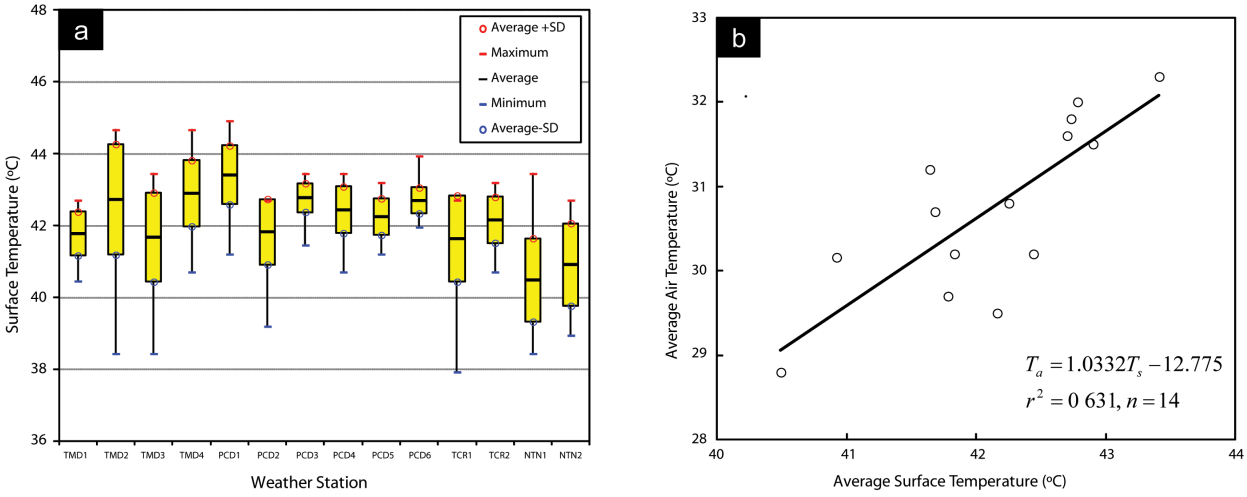

Figures 10. (a.) Surface temperature of source area around the weather stations, and (b.) The relationship between air temperature (T_a) obtained from the reference weather stations and average surface temperature (T_s) derived from the thermal infrared image of Landsat TM data on April 25, 2009.

Spatial patterns of air temperature were investigated with the Landsat TM thermal image acquired on April 25th, 2009 and the result of the isothermal color ramp at one degree of temperature presented in Figure 11a. In the BMA, most parcels having high T_a values are associated with high-density built-up land. Parcels having low T_a values are located outside the urban area. Most parcels having relatively high T_s values are found in urban areas. However, a few high T_s parcels were located in rural areas. Generally, the magnitudes of T_a are strongly related to regional T_s characteristics. For the estimating the temporal characteristics of the urban heat island intensity (UHII) in BMA (Figure 11b). The UHII reached a maximum of 9°C on the diurnal range of April 25th, 2009.

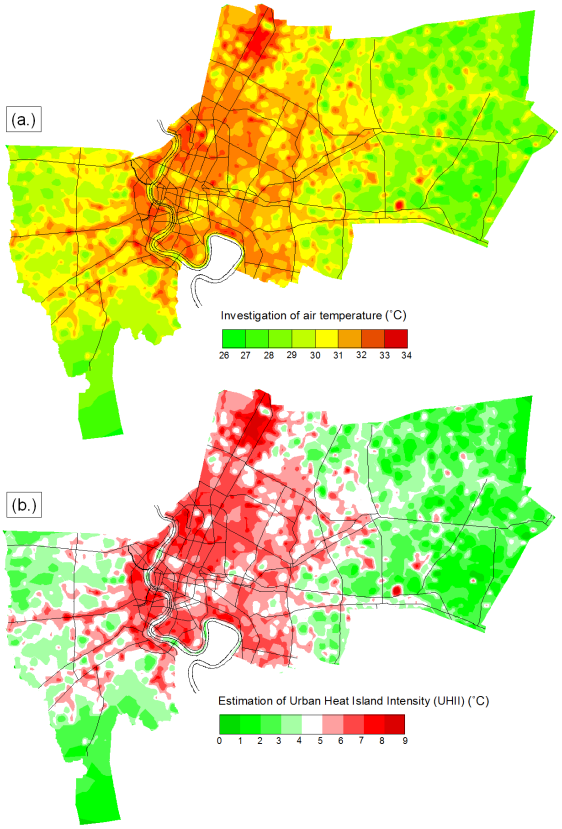

Figures 11. (a.) Investigation of air temperature (T_a) derived from Landsat TM thermal infrared image on April 25th, 2009 and (b.) Estimation result of the urban heat island intensity (UHII) on April 25th, 2009.

5. Conclusions

The aim of this study was to quantify UHIs and understand the different approaches that are used in indicator development. It is essential to distinguish between UHIs that are quantified from (a) air temperatures and (b) land surface temperatures (LSTs). Surface temperature data for SUHI quantifications originate from satellite-borne sensors. These sensors measure the temperature of the land surface as seen from above, and this temperature is related to the air temperature in the same location. Therefore, this paper proposed the term surface urban heat island (SUHI) for a UHI that is measured with LST.

Greater density, a reduction in open spaces and green cover, and the growth of built up space have been shown to increase the heat island phenomenon. These thermal changes deteriorate the urban environment, causing health problems. Therefore urban planners, designers, and architects need to consider the urban climate while designing and planning cities. This study has demonstrated the use of Landsat TM thermal remote sensing to observe and assess SUHIs in BMA, Thailand. Changes in land use and land cover were accompanied by changes in SUHI. From 1994 to 2009, the urban or built-up surface temperature increased in all zone areas of the BMA, and continued to increase between 1994, 2000 and 2009. Moreover, temperature differences between the urban area and the surrounding rural areas significantly widened, especially in the inner and middle zones. This could lead to an intensified urban heat island effect in the urban areas. The results of this study can provide methods and basic information for the reduction of SUHI and the establishment of environmentally friendly urban planning.

All the analyses in this paper were based on the interpretation of remote sensing images and the results showed that remote sensing images are ideal for analyzing SUHI, by which we analyzed not only the phenomenon of SUHI but the impact factors of SUHI from the regional level to the local level. Several limitations of the surface temperature measurements taken by remote sensing should be mentioned. First, they do not fully capture radiant emissions from vertical surfaces, such as a building's wall, because the equipment mostly observes emissions from horizontal surfaces such as streets, rooftops, and treetops. Second, remotely sensed data represent radiation that has traveled through the atmosphere twice, as wavelengths travel from the sun to the earth as well as from the earth to the atmosphere. Thus, the data must be corrected to accurately estimate surface properties including solar reflectance and temperature.

In future studies, there is the need to focus on: (i) the impact of the distribution pattern of different land use and land cover (LULC) types on SUHI; (ii) more accurate estimation of the variable conditions of LULC types; (iii) comparison of SUHIs estimated for cities of different sizes under different climatic conditions; and (iv) multi-temporal studies of SUHIs of a single city over four seasons using different satellite data.

Acknowledgements

The authors would like to express their sincere thanks to the anonymous reviewers for their constructive suggestions, comments, and help. This research is supported by the Department of Civil Engineering and Architecture, Graduate School of Science and Engineering, Saga University, Japan and Geo-Informatics and Space Technology Development Agency (Public Organization): GISTDA, Thailand.

References

Aires, F., Prigent, C., Rossow, W. B. & Rothstein, M. (2001). A new neural network approach including first-guess for retrieval of atmospheric water vapor, cloud liquid water path, surface temperature and emissivities over land from satellite microwave observations. *J. Geophys. Res.,* 106, 14887-14907.

Akbari, H., Rosenfeld, A., Taha, H., & Gartland, L. (1996). Mitigation of summer urban heat islands to save electricity and smog. In *76th Annual American Meteorological Society Meeting Atlanta*, GA.

Akbari, H., Pomerantz, M., & Taha, H. (2001). Cool surfaces and shade trees to reduce energy use and improve air quality in urban areas. *Solar Energy*, 70, 295-310.

Arnfield, A. J. (2003). Two decades of urban climate research: A review of turbulence, exchanges of energy and water, and the urban heat island. *Int. J. Climatol.* 23, 1-26.

Balling, R. C., & Brazell, S. W. (1988). High resolution surface temperature pattern in a complex urban terrain. *Photogrammetric Engineering and Remote Sensing,* 54, 1289-1293.

Buyantuyev, A., & Wu, J. (2010). Urban heat islands and landscape heterogeneity: Linking spatiotemporal variations in surface temperatures to land cover and socioeconomic patterns. *Landscape Ecology, 25*(1), 17-33.

Boonjawat, J., Niitsu, K., & Kubo, S. (2000). *Urban heat island: Thermal pollution and climate change in Bangkok*. Report of the Southeast Asia START Regional Center. Retrieved from http://www.start.or.th/heatisland/

Barsi, J. A., Schott, J. R., Palluconi, F. D., Helder, D. L., Hook, S. J., Markham, B. L., Chander, G. & O'Donnell, E. M. (2003). Landsat TM and ETM+ thermal band calibration. *Canadian Journal of Remote Sensing, 29*(2), 141-153.

Ben-Dor, E., & Saaroni, H. (1997). Airborne video thermal radiometry as a tool for monitoring microscale structures of the urban heat island. *International Journal of Remote Sensing, 18*(4), 3039-3053.

Buyantuyev, A., & Wu, J. (2010). Urban heat islands and landscape heterogeneity: Linking spatiotemporal variations in surface temperatures to land-cover and socioeconomic patterns. *Landscape Ecology, 25*(1), 17-33.

Chen, Y., Wang, J., & Li, X. (2002). A study on urban thermal field in summer based on satellite remote sensing. *Remote Sensing for Land and Resources,* 4, 55-59.

Chen, X. L., Zhao, M. Z., Li, P. X., & Yin, Z. Y. (2006). Remote sensing image-based analysis of the relationship between urban heat island and land use/cover changes. *Remote Sensing of Environment,* 104, 133-146.

Chander, G., & Markham, B. (2003). Revised Landsat-5 TM radiometric calibration procedures and post-calibration dynamic ranges. *IEEE Transactions on Geoscience and Remote Sensing, 41*(11), 2674-2677.

Frey, C. M., Rigo, G., & Parlow, E. (2007). Urban radiation balance of two coastal cities in a hot and dry environment. *International Journal of Remote Sensing, 28*(12), 2695-2712.

Forman, R. T. T. (1995). *Land mosaics: The ecology of landscape and regions.* NY: Cambridge University Press.

Gallo, K. P., Tarpley, J. D., McNab, A. L., & Karl, T. R. (1995). Assessment of urban heat islands: A satellite perspective. *Atmospheric Research,* 37, 37-43.

Gallo, K. P., & Owen, T. W. (1998a). Assessment of urban heat island: A multisensory perspective for the Dallas-Ft. Worth, USA region. *Geocarto International,* 13, 35-41.

Gallo, K. P., & Owen, T. W. (1998b). Satellite-based adjustments for the urban heat island temperature bias. *Journal of Applied Meteorology,* 38, 806-813.

Gustafson, E. J. (1998). Quantifying landscape spatial pattern: What is the state of the art? *Ecosystems,* 1, 143-156.

Kiattiporn, W., Somchai, M., Nipon, K., & Wattanapong R. (2008). The impacts of climatic and economic factors on residential electricity consumption of Bangkok Metropolis. *Energy and Buildings,* 40, 1419-1425.

Leitao, A. B., Miller, J., Ahern, J., & Mc Garigal, K. (2006). *Measuring landscapes: A planner's handbook.* Washington, DC: Island Press.

Lu, D., & Weng, Q. (2006). Spectral mixture analysis of ASTER images for examining the relationship between urban thermal features and biophysical descriptors in Indianapolis, United States. *Remote Sensing of Environment, 104*(2), 157-167.

Lo, C. P., Quattrochi, D. A., & Luvall, J. C. (1997). Application of high-resolution thermal infrared remote sensing and GIS to assess the urban heat island effect. *International Journal of Remote Sensing,* 18, 287-304.

Liang, B., & Weng, Q. (2008). Multi-scale analysis of census-based land surface temperature variations and determinants in Indianapolis, United States. *Journal of Urban Planning D-ASCE, 134*(3), 129-139.

Nichol, J. E. (1994). A GIS-based approach to microclimate monitoring in Singapore's high-rise housing estates. *Photogrammetric Engineering and Remote Sensing,* 60, 1225–1232.

Nichol, J. E., Fung, W. Y., Lam, K., & Wong, M. S. (2009). Urban heat island diagnosis using ASTER satellite images and 'in situ' air temperature. *Atmospheric Research, 94*(2), 276-284.

Oke, T. R. (2004). Initial guidance to obtain representative meteorological observations at urban sites. IOM Report 81, *World Meteorological Organization,* Geneva.

Oke, T. R. (1982). The energetic basis of the urban heat-island. *QJRMS,* 108, 1-24.

Owen, T. W., Carlson, T. N., & Gillies, R. R. (1998). An assessment of satellite remotely-sensed land cover parameters in quantitatively describing the climatic effect of urbanization. *International Journal of Remote Sensing,* 19, 1663-1681.

Poumadere, M., Mays, C., LeMer, S., & Blong, R. (2005). The 2003 heat wave in France: Dangerous climate change here and now. *Risk Annual, 25*(6), 1483-1494.

Pu, R., Gong, P., Michishita, R., & Sasagawa, T. (2006). Assessment of multi-resolution and multi-sensor data for urban surface temperature retrieval. *Remote Sensing of Environment,* 104, 211-225.

Quattrochi, D. A., & Luvall, J. C. (1999). Thermal infrared remote sensing for analysis of landscape ecological processes: Methods and applications. *Landscape Ecology, 14*(6), 577-598.

Rao, P. K. (1972). Remote sensing of urban "heat islands" from an environmental satellite. *Bulletin of the American Meteorological Society,* 53, 647-648.

Roth, M., Oke, T. R., & Emery, W. J. (1989). Satellite-derived urban heat islands from three coastal cities and the utilization of such data in urban climatology. *Int. J. Remote Sens.,* 10, 1699-1720.

Streutker, D. R. (2002). A remote sensing study of the urban heat island of Houston, Texas. *International Journal of Remote Sensing, 23*(13), 2595-2608.

Stewart, I. D. (2011). A systematic review and scientific critique of methodology in modern urban heat island literature. *IJCli,* 31, 200-217.

Sun, D., & Pinker, R. T. (2003). Estimation of land surface temperature from a Geostationary Operational Environmental Satellite (GOES-8), *J. Geophys. Res.,*108, 4326-4241.

Schroeder, T. A., et al. (2006). Radiometric correction of multi-temporal Landsat data for characterization of early successional forest patterns in western Oregon. *Remote Sensing of Environment,* 103, 16-26.

Peng, S., et al. (2011). Surface urban heat island across 419 global big cities. Environ. *Sci.&Technol,* 46, 696-703.

Turner, M. G. (2005). Landscape ecology: What is the state of the science? *Annual Review of Ecological Evolution and Sensing*, 36, 319–344.

Voogt, J. A., & Oke, T. R. (2003). Thermal remote sensing of urban areas. *Remote Sensing of Environment*, 86, 370-384.

Voogt, J. A. (2004). *Urban Heat Islands: Hotter Cities.* Retrieved from http://www.actionbioscience.org/environment/voogt.html

Weng, Q. (2001). A remote sensing-GIS evaluation of urban expansion and its impact on surface temperature in Zhujiang Delta, China. *International Journal of Remote Sensing, 22*(10), 1999-2014.

Weng, Q. (2003). Fractal analysis of satellite-detected urban heat island effect. *Photogrammetric Engineering and Remote Sensing, 69*(5), 555–566.

Weng, Q. (2009). Thermal infrared remote sensing for urban climate and environmental studies: Methods, applications, and trends. *ISPRS Journal of Photogrammetry and Remote Sensing,* 64, 335–344.

Wang, J., Rich, P. M., Price, K. P., & Kettle, W. D. (2004). Relations between NDVI and tree productivity in the central Great Plains. *International Journal of Remote Sensing, 25*(16), 3127-3138.

White, M. A., Nemani, R. R., Thornton, P. E., & Running, S. W. (2002). Satellite evidence of phonological differences between urbanized and rural areas of the eastern United States deciduous broadleaf forest. *Ecosystems,* 5, 260–277.

Weng, Q., Lu, D., & Schubring, J., (2004). Estimation of land surface temperature vegetation abundance relationship for urban heat island studies. *Remote sensing of Environment, 89*(4), 467-483.

Xiao, R., Weng, Q., Ouyang, Z., Li, W., Schienke, E., & Zhang, Z. (2008). Land surface temperature variation and major factors in Beijing, China. *Photogrammetric Engineering and Remote Sensing, 74*(4), 451–461.

Yuan, F., Sawaya, K. E., Loeffelholz, B. C., & Bauer, M. E. (2005). Land cover mapping and change analysis in the Twin Cities Metropolitan Area with Landsat remote sensing. *Remote Sensing of Environment, 98*(2.3), 317-328.